Edge based features for content based image retrieval

Minakshi Banerjee [1], Malay K. Kundu*

Machine Intelligence Unit, Indian Statistical Institute, 203, B. T. Road, Kolkata 700 108, India

Abstract

The common problem in content based image retrieval (CBIR) is selection of features. Image characterization with lesser number of features involving lower computational cost is always desirable. Edge is a strong feature for characterizing an image. This paper presents a robust technique for extracting edge map of an image which is followed by computation of global feature (like fuzzy compactness) using gray level as well as shape information of the edge map. Unlike other existing techniques it does not require pre segmentation for the computation of features. This algorithm is also computationally attractive as it computes different features with limited number of selected pixels.

Keywords: Plateaus; Fuzzy compactness; Connectedness; Candidate pixels; Fuzzy set

1. Introduction

Content based image retrieval (CBIR) techniques are becoming increasingly important in multimedia information systems. A key building block in an image retrieval system is image indexing (automatically or manually). Indexing means characterization of images based on one or more image properties. CBIR uses [1] an automatic indexing scheme where implicit properties of an image can be included in the query to reduce search time for retrieval from a large database. Features like color, texture, shape, spatial relationship among entities of an image and also their combination are generally being used for the computation of multidimensional feature vector. The features color, texture, shape are known as primitive features. Our proposed work is based on one such primitive feature and can be used in the lowest level of query [2]. Other type of feature includes semantic feature which characterizes an event as depicted in an image. Recent trend in CBIR research is to develop efficient features for simpler characterization of images and related matching techniques so that it can handle real life images. Pre segmentation is necessary whenever a scene is characterized by different objects in it. Segmentation becomes less important when there are large number of fragmented objects in a scene or no specific objects. The cost of computation depends upon the method used, whereas accuracy depends upon the a priori information of the total number of classes present in the scene. In the proposed technique no apriori information of the classes are necessary. There are methods [3–5] in which edge points of a scene can be used for indexing images. Edges characterizes gray level discontinuities of an image. Edges that are due to discontinuities between the regions are generally of strong value. Edges that are due to variation within regions and also due to defects of imaging give rise to weak edges. Region boundaries are characterized by strong edges and approximately represent the shape of the regions. Using directional histogram of edge Jain and Vailaya [3] proposed a technique for shape comparison. It is well known that in histogram comparison, dissimilar images can also give rise to similar histograms. Ravela et al. proposed a method to characterize visual appearance for determining global similarity in images with geometric

* Corresponding author. Tel.: +91-33-577-4906; fax: +91-33-577-6680.

E-mail addresses: minakshi_r@isical.ac.in (M. Banerjee), malay@isical.ac.in (M.K. Kundu).

[1] Minakshi Banerjee is grateful to the Council of Scientific and Industrial research, New Delhi, India, for providing her a research fellowship vide, grant (no.9/93(60)/99-EMR.I) to carry out her research work.

features [6]. Zhou and Huang [4] proposed structural features extracted from edge maps for CBIR. Histogram of blurred images are also used for defining shape features because histograms of blurred images are strongly influenced by the original shapes of different regions in it [7]. Bruno et al. [8] defined multiscale families of feature calculated from the convolution of the input image with a set of multiscale Gaussian function. Using recent edge detection method, Wang et al. [5] presented a technique in which edges of the images can be extracted by wavelet transform. The edge images are then classified based on the invariant moments.

Although minimum number of features are always desirable property for characterizing images but a single feature may not be sufficient for achieving desired accuracy. Colour and texture based similarity measures without shape information failed to produce desired results. Combining shape and color in invariant fashion have been reported in [9]. Achard et al. proposed a shape based feature combining gray level information [10] by thresholding the image at different gray level. Compactness of the object is computed over each gray level for shape comparison. This method is computationally very expensive and cost is proportional to the number of gray levels considered.

It is also desirable that, the selected features should not be computationally expensive, should be noise tolerant and invariant to rotation, translation and scaling. Keeping these points in view the major contributions in this paper are as follows:

We have used the blurred image as input and used the concept of Top and Bottom of the intensity surface to extract possible candidates for the edge map. This map is converted to fuzzy gradient map by measuring the relative intensity difference over small neighbourhood.

Multilevel thresholding is performed to find multilevel fuzzy edge map from which (fuzzy compactness) is computed. This feature is invariant to Rotation Translation and Scaling by definition. The feature vector elements include fuzzy compactness value of the edge map obtained at different level which is used to compute the degree of similarity measure of an image with the query image for image retrieval.

The paper is organized as follows:

Section 2 describes briefly the mathematical model used in this work. Section 3 describes implementation and used algorithm. Section 4 describes the experimental results. Section 5 gives a conclusion.

2. Image representation and properties used for proposed CBIR

In this section, membership functions used in fuzzy set theoretic approach and some of the geometrical properties of regions and their modified version used in the experiment have been discussed. Here the feature vectors are computed using fuzzy set theoretic approach. Gray level images are inherently fuzzy in nature due to the uncertainty that exists in locating the exact position of the boundary which separates the object from background. Even for perfectly homogeneous objects the corresponding images will have graded composition of gray levels [11] due to imperfection of imaging. Hence fuzzy set theoretic approach will be appropriate to handle such uncertainties.

2.1. Image as fuzzy sets

An image X of $M \times N$ dimension and L levels can be considered [12] as an fuzzy subset A' in a space of points $X = \{x\}$. Each point in X can be characterized by a membership function $\mu_A(x_{mn})$ which can have a value in the interval [0,1]. $\mu_A(x_{mn})$ denotes the degree to which an event x_{mn} belong two A'.

It is convenient to express the membership function in terms of standard S type or Π type function. The functions are as follows:

Standard S function is given by

$$S(x;a,b,c) = \begin{cases} 0 & x \leqslant a, \\ 2 \times \{\frac{(x-a)}{(c-a)}\}^2 & a \leqslant x \leqslant b, \\ 1 - 2 \times \{\frac{(x-c)}{(c-a)}\}^2 & b \leqslant x \leqslant c, \\ 1 & x \geqslant c. \end{cases} \quad (1)$$

Standard Π function is given by

$$\Pi(x;b,c) = \begin{cases} S(x;c-b,c-b/2,c) & x \leqslant c, \\ 1 - S(x;c,c+b/2,c+b) & x \geqslant c. \end{cases} \quad (2)$$

It should be mentioned that the assignment of the membership is subjective in nature and reflects the context at which the problem is viewed. Other form of membership function exponential in nature [13] given as

$$\mu(x) = \exp[-d(X,C)], \quad (3)$$

where $d(X,C)$ is the distance of an element with feature vector $X = [x_1, x_2, \ldots, x_n]$ from a prototype $C = [c_1, c_2, \ldots, c_n]$ of a class and $d(X,C) \geqslant 0$. The availability of the mathematical function depends upon the nature of the prototype.

2.1.1. Fuzzy geometrical properties

Rosenfield [14] proposed certain Geometrical properties based on fuzzy set theoretic approach for characterizing regions of an image. Of them the concept of connectedness has been used in our experiment.

Degree of connectedness: let μ be a mapping from S into [0, 1] i.e., a fuzzy subset of S. Let $\rho : P = p_0, p_1, \ldots, p_n = Q$ be any path between two points (P,Q) of S. The path strength $s_\mu(\rho)$ of ρ with respect to μ is defined as

$$s_\mu(\rho) = \min_{0 \leqslant i \leqslant n} \mu_\rho(p_i). \quad (4)$$

The Degree of connectedness of P and Q with respect to μ is defined as

$$C_\mu(P,Q) = \max_\rho(s_\mu(\rho)), \tag{5}$$

where max is taken over all paths from P to Q.

Proposition 1. *If μ is into $[0,1]$ and $S = \mu^{-1}(1)$ i.e., $\{P \mid P \in S \text{ and } \mu(p) = 1\}$ then $\mu(\rho) = 1$ consists entirely of points of S and $C_\mu(P,Q) = 1$ if there exists a path from P to Q all of whose points are mapped to 1 by some property in μ. This condition generalizes the non-fuzzy concept of connectedness.*

Fuzzy Compactness: For a $M \times N$, μ_{mn} array the fuzzy compactness $comp(\mu)$ is defined as [15].

$$comp(\mu) = \frac{a(\mu)}{p^2\mu}, \tag{6}$$

where $a(\mu)$ and $p(\mu)$ are the fuzzy area and perimeter of (μ), respectively. Where $a(\mu)$ and $p(\mu)$ are given by Eqs. (7) and (8)

$$a(\mu) = \sum_m \sum_n \mu_{mn}, \tag{7}$$

$$p(\mu) = \sum_{m=1}^{M} \sum_{n=1}^{N-1} |\mu_{mn} - \mu_{m,n+1}| + \sum_{n=1}^{N} \sum_{m=1}^{M-1} |\mu_{mn} - \mu_{m+1,n}|. \tag{8}$$

For example we consider a 4×4 μ_{mn} array

$$\begin{bmatrix} 0 & 0 & 0 & 0 \\ 0 & \alpha & \beta & 0 \\ 0 & 0 & \beta & \gamma \\ 0 & \delta & 0 & 0 \end{bmatrix},$$

here $\alpha(\mu) = \alpha + 2\beta + \gamma + \delta$ and $p(\mu) = [\alpha + |\beta - \alpha| + \beta + \beta + |\gamma - \beta| + \delta + \delta] + [\alpha + \alpha + \delta + \beta + 0 + \beta + \gamma + \gamma]$ where $\alpha, \beta, \gamma, \delta$ are the membership values with $1 \geqslant \alpha, \beta, \gamma, \delta \geqslant 0$.

2.2. Proposed technique for CBIR

The proposed feature extraction technique could be explained using the building block shown in Fig. 1. Before explaining the actual method we like to define different formulations and definitions used in the proposed work.

2.2.1. Identification of extremas

(Plateau Top and Plateau Bottom)

Edges in an image are the transitions between two uniform intensity surfaces. The uniform intensity surfaces are defined in terms of *Plateaus*. Plateaus are defined as connected subsets of uniform intensity pixels. This definition can be taken as the special case of *fuzzy plateaus* introduced by Rosenfield [14].

Plateau: Let S denote the set of all pixels in an image. By a plateau in S is meant a maximum connected subset S_p on which the intensity has a constant value. In other words $S_p \in S$ is a Plateau iff

(i) S_p is connected, (ii) $I(P) = I(Q)$ for all $P, Q \in S_p$, (iii) $I(P) \neq I(Q)$ for all pair of neighbouring points $P \in S_p$ and $Q \notin S_p$.

Clearly $P \in S$ belongs to one Plateau.

We call the Plateau S_p a Top if it's gray value is a local maximum i.e. $I(P) \geqslant I(Q)$ for all pairs of neighbouring point $P \in S_p$ and $Q \notin S_p$. Similarly we call S_p a Bottom if it's gray value is a local minimum. The gray values of all elements of *Plateau Top* is greater than the gray value of any element of the border and the gray values of any element of a *Plateau Bottom* is less than gray values of the border. Let S_{pt} be a Plateau Top and S_{pb} a Plateau Bottom. The pixels in border region $B(S_{pt}, S_{pb})$ between a Plateau Top and Plateau Bottom can be defined as the points which are eight neighbours of at least one element of S_{pt}, S_{pb}. Considering a 3×3 neighbourhood around a pixel Uma Shankar et al. proposed a method for characterizing extreme components of an image [16]. The pixels are labeled as pels of a (a) *Plateau Top* for which the pixel is greater or equal to maximum in it's 3×3 neighbourhood. (b) *Plateau Bottom* for which pixels are less or equal to minimum in it's 3×3 neighbourhood. (c) The remaining pels are *Candidate pels* for forming fuzzy gradient map.

$$\begin{bmatrix} 2 & 4 & 8 \\ 3 & \mathbf{8} & 7 \\ 6 & 6 & 6 \end{bmatrix} \text{ Plateau Top,}$$

$$\begin{bmatrix} 4 & 2 & 3 \\ 6 & \mathbf{2} & 3 \\ 5 & 4 & 2 \end{bmatrix} \text{ Plateau Bottom,}$$

$$\begin{bmatrix} 2 & 4 & 8 \\ 4 & \mathbf{8} & 9 \\ 7 & 7 & 9 \end{bmatrix} \text{ Candidate pel.}$$

2.2.2. Membership formulation

Membership function $\mu_m(P)$ for determining fuzzy gradient map: We have used the modified form of membership function of Eq. (3) for our problem. The border region of the plateaus of the blurred (gaussian) image is taken as input for finding the fuzzy gradient map and the total dynamic range of 0 to 256 is considered. Around each candidate pixel the neighbouring pixels are situated in eight distinct directions at a step of 45°. The line joining two opposite pixels which makes four distinct lines are considered. The gradient membership function for an edge point is given in equation below

$$\mu_m(P) = k_m \exp(-x). \tag{9}$$

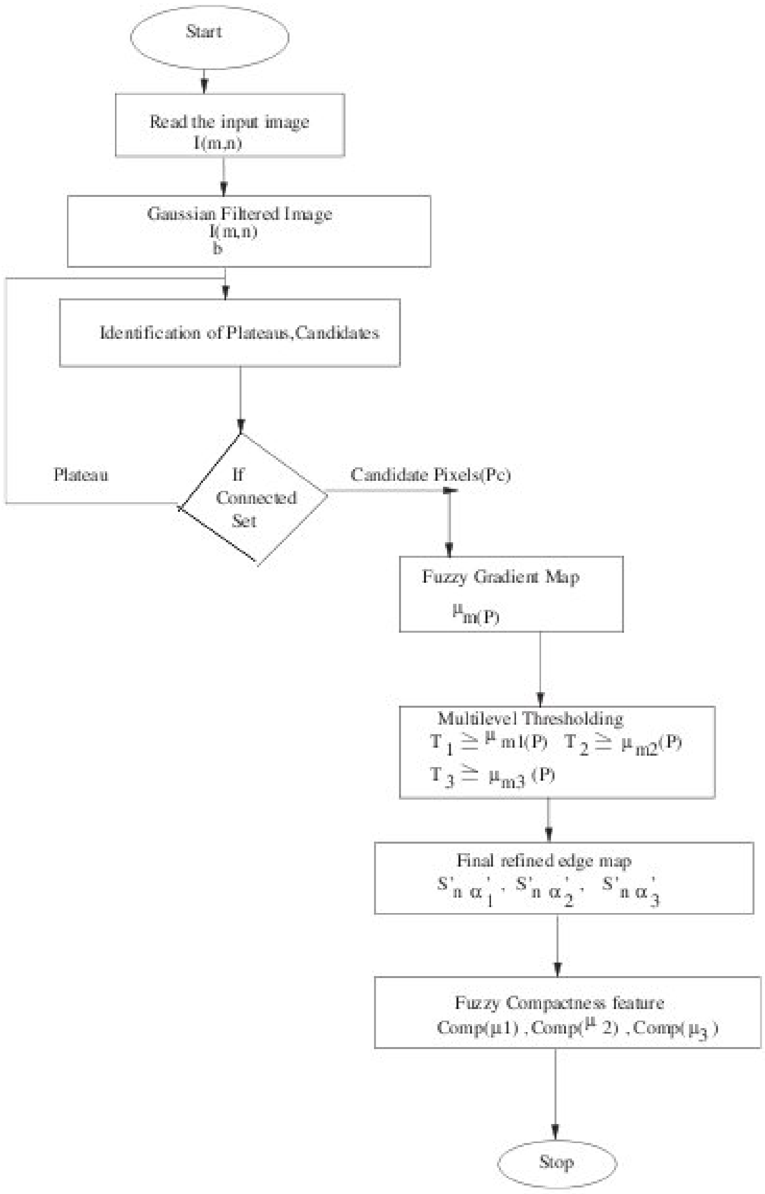

Fig. 1. Flow chart for proposed feature extraction.

Considering Fig. 2, if d_{ac} is the gray level difference between the opposite neighbours about the candidate pixel in a direction say, $(0,4)$ and d_{al} is the gray level difference in the perpendicular direction say $(2,6)$ then $x=(1+d_{al})/(1+d_{ac})$. We compute the magnitude membership values in four direction pairs. The maximum value out of the four directions is assigned to the candidate pixel. Let I_{mn} be the gray level of the point $P(m,n)$. If $d_{al} = |I_{m,n-1} - I_{m,n+1}|$ then $d_{ac} = |I_{m-1,n} - I_{m+1,n}|$ vice-versa as shown in Fig. 2.

The value of k_m can be estimated from the following condition. $\mu_m(P)$ is ranging from [0,1]. Minimum value of $d_{al} = 0$ and maximum value of d_{ac} say L should map the membership value to into 1. Different values of L should give rise to different value of k_m hence different crossover point ($\mu_m(P) = 0.5$). The strongest edge pixel at any point (m,n) is supposed to possess gray level difference $\simeq 256$ in one direction and nearly zero in it's perpendicular direction and the edge should points along the minimum difference direction. Putting $d_{ac} = 255$ and $d_{al} = 0$ in Eq. (9) value of k_m obtained is $\simeq 1.0039$. Higher membership value characterizes strong edge pixels, and lower membership values will characterizes weak edge pixels shown in Fig. 3 if they

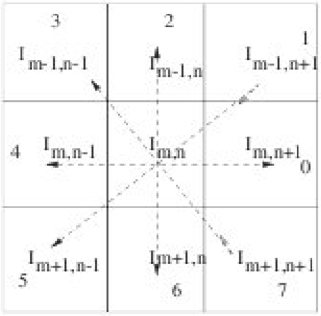

Fig. 2. 3×3 neighbourhood of the candidate pixel.

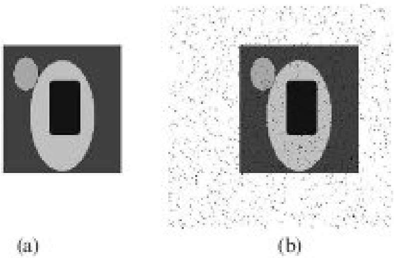

Fig. 3. (a) Original image and (b) noise introduced.

are already present in the image. Changing the value k_m by a factor is in effect changing the pixel contrast [13] i.e., transforming the membership value $T_1(\mu(P)) = T'(\mu(P))$.

Membership function $\mu_d(P)$ for determining connectedness of the edge points: The membership for connectedness is represented by an exponential function. We consider a $M \times N$, $\mu_m(P)$ array. In the neighbourhood of a pixel $p(m,n)$ if there exits a pixel $p(m',n')$ such that,

$$|\mu_{mn} - \mu_{m'n'}| \leqslant T, \tag{10}$$

where (T is the non-negative threshold) are considered similar in magnitude. Again if

$$|ang(m,n) - ang(m',n')| \leqslant A \tag{11}$$

(where A is the angle threshold) are considered similar in direction [17]. The two above properties are combined to link similar pixels and the degree of linking is expressed by a new membership function as expressed in Eq. (12).

The number of pixels possessing $\mu_m(P)$ above some threshold value ($\geqslant 0.5$) and $\leqslant 1.0$ and simultaneously having directions which didn't differ more than 45° in a neighbourhood of 3×3 or 5×5 window size are counted. The membership function is of the form

$$\mu_d(P) = k_d \exp(-x), \tag{12}$$

where $x = 1/(n1 + n2 + n3)$.

$n1$ denotes the number of edge pixels possessing same angle to that of the candidate pel, $n2$ is the number of edge pixels having $+45^\circ$ difference with the candidate pixel, $n3$ is the number of edge pixels having angle -45° difference with the candidate pixel. The value of k_d is estimated by the maximum number of connected pixels say K along any of the four directions within the defined window. With $x = 1/K$ maps the membership to 1. Changing the value of k_d will in effect change the number of connected pixels over a defined window.

2.2.3. Similarity metric

Euclidean distance metric is used to compute the dissimilarity value between two feature vectors. If $X = [x_1, x_2, \ldots, x_l]$ and $Y = [y_1, y_2, \ldots, y_l]$ are two feature vectors then the Euclidean distance metric between X, Y is given by,

$$E_d = \sqrt{\sum (x_i - y_i)^2}. \tag{13}$$

2.2.4. Performance evaluation

To evaluate the performance of retrieval we consider the standard retrieval benchmarks such as *recall rate* and *precision rate* [18]. Let n_1 be the number of images retrieved in top 20 positions that are close to the query. Let n_2 represent the number of images in the data base similar to the query. Evaluation standards *recall rate* and *precision rate* are defined as follows:

$$Recall\ rate = \frac{n_1}{n_2} \times 100\%, \tag{14}$$

$$Precision\ rate = \frac{n_1}{20} \times 100\%. \tag{15}$$

2.2.5. Building block

The flowchart for the proposed feature extraction process is shown in Fig. 1.

The intensity image matrix $I(m,n)$ is convolved with Gaussian function and resulted into a blurred image matrix $I_b(m,n)$

$$I_b(m,n) = I(m,n) * G(x,y), \tag{16}$$

where $G(x,y) = (1/\sqrt{2}\pi\sigma)e^{-(x^2+y^2)/2\sigma^2}$ where σ effectively determines the window size of the filter which in turn determines the degree of smoothing. The blurred image preserves the original shape. By gaussian filtering, part of the intensity is distributed to the neighbours while preserving the edge information. The border region which characterizes the transition between two uniform Plateaus could be determined from the blurred image. We are interested in finding the transition between the Plateau regions consisting of the possible edge candidates P_c which acts as an input for finding the fuzzy gradient map. The points of this region are characterized by $\mu_m(P)$ representing the edge strength in the interval [0,1]:

$$s_n = \{(\mu_m, P_c)\}. \tag{17}$$

The gradient map $\mu_m(P)$ is thresholded at different levels using ($\alpha - cut$) [13] with membership values greater from

0.5 onwards. Let the candidates of the multilevel gradient map be represented by

$$s_{n\alpha} = \{(P \in s_n:\ \mu_m(P) \geqslant \alpha\}, \tag{18}$$

where $0.5 \geqslant \alpha \leqslant 1$.

Now $s_{n\alpha}$ is taken as input to find out the refined edge map using the notion of highest connectivity which resulted in a subset $s'_{n\alpha}$ as shown in Eq. (19). Points which are preserving highest connectivity within a defined window are extracted using the membership function $\mu_d(P)$ shown in Eq. (12).

$$s'_{n\alpha} = \{(x \in s_{n\alpha}:\ \mu_d(P) \geqslant \alpha'\} \tag{19}$$

α' is $\simeq 1$ to change the degree of connectivity between the adjacent pixels to the highest value (Proposition 1 of Eq. (5)).

Fuzzy compactness feature $comp(\mu)$ is computed on $s'_{n\alpha}$ using Eq. (6).

3. Algorithm and implementation details

Algorithm. *Step* 1: Gaussian filtering is performed on the image.

Step 2: Each pixel is labeled as (a) Plateau Top or maxima or (b) Plateau Bottom or minima or (c) Candidate pel.

Step 3: If the labeled pixel is a candidate pel, its gradient membership value $\mu_m(P)$ and its edge direction is estimated. The points thresholded above different membership values ($\mu_m(x) \geqslant 0.5$) are selected.

Step 4: Candidate pixels similar in edge magnitude and direction are linked.

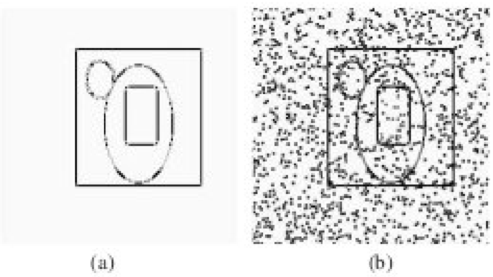

Fig. 4. Multilevel gradient map thresholded at $\mu_m(P) \geqslant$ (a) 0.6 and (b) 0.6.

Step 5: Fuzzy compactness feature vector is computed from the edge map.

Step 6: Euclidean distance is computed between the feature vector elements of the query image and images in the database and ranked according to distance.

Feature vector element comprising of [$comp(\mu_1)$, $comp(\mu_2)$, $comp(\mu_3)$] is computed using Eq. (6). Two set of features(fuzzy compactness value of the edge map) at different threshold have been computed separately for studying retrieval performance with different window size.

Features: The schematic diagram for feature extraction is shown in Fig. 1.

Feature set (A) (for 3×3 window size):

$comp(\mu_1)$ is computed from the edge map by thresholding at $\mu_m(P) \geqslant 0.6$.

$comp(\mu_2)$ is computed from the edge map obtained by thresholding at $\mu_m(P) \geqslant 0.7$.

$comp(\mu_3)$ is computed from the edge map obtained by thresholding at $\mu_m(P) \geqslant 0.8$.

These set of features are computed using the value of $k_m \simeq 1.0039$ as shown in Eq. (9) and value of k_d is determined from Eq. (12) over 3×3 window size. The corresponding edge maps of Fig. 3(a) and Fig. 7 are shown in Fig. 5 and Fig. 8, respectively.

Feature set (B):

$comp(\mu_1)$ is computed from the enhanced map thresholded at $\mu_m(P) \geqslant 0.8$

$comp(\mu_2)$ is computed from the enhanced map thresholded at $\mu_m(P) \geqslant 0.9$.

Using the value of $k_m \simeq 1.18$ and value of k_d as determined from Eq. (12) over 5×5 window size, the feature elements $comp(\mu_1)$ and $comp(\mu_2)$ are computed. The edge map of Fig. 7(a) obtained using feature set (B) with gradient membership $\mu_m(P) \geqslant 0.8$ is shown in Figs. 9(a2) and the edge map with $\mu_m(P) \geqslant 0.8$ obtained using feature set (A) is shown in Fig. 9(a).

$comp(\mu_3)$ is computed from the edge map obtained by thresholding at $\mu_m(P) \geqslant 0.7$ with $k_m \simeq 1.18$. Only those pixels are selected as candidates which are having other pixels in the direct neighbourhood with gradient membership $\mu_m(P)$ greater than 0.7. The value of K in this case is the maximum number of such pixels in 3×3 window and k_d is determined with the value of K using Eq. (12). The

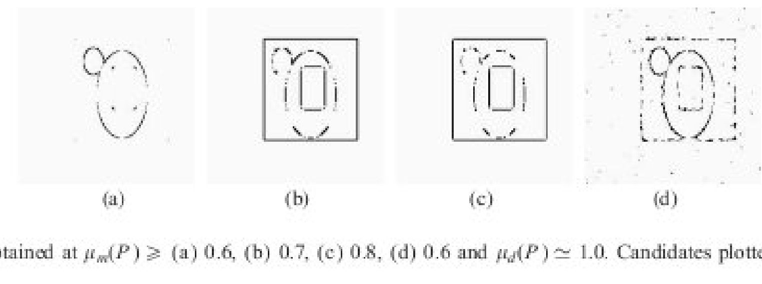

Fig. 5. Edge map obtained at $\mu_m(P) \geqslant$ (a) 0.6, (b) 0.7, (c) 0.8, (d) 0.6 and $\mu_d(P) \simeq 1.0$. Candidates plotted as crisp edge point.

corresponding edge maps of Fig. 3(a) and Figs. 7(b), (c), are shown in Figs. 6 and 10 respectively.

Although we have selected three thresholding levels of membership but the variation of selection of thresholding level will not change the result drastically. Low, medium, high types of edge strength are grouped in three distinct categories. Value of k_m and k_d can be tuned to select different candidates based on their weighted membership value.

4. Experimental results

We have performed our experiment using two databases of which the first database consists of 120 gray level images (256×256) of different objects downloaded mainly from Google engine (www.google.com), OlivettiFace database(*ftp://ftp.uk.research.att.com:pub/data/att_faces.tar.Z*) and some synthetically generated images. The images in this database are mainly of single object both with textured and non-textured background. This collection consists of dissimilar group of images of which each group is having some similarity within itself. Such database consisting of both visually distant set of images as well as closely related images are useful in studying the system performance properly [19]. The second database consists of the trade mark and logo images of United States and Patent and Trademarks office (USPTO) consisting of 1053 binary images. The images are converted to gray level and reduced to (256×256) for the experiment. The size of the gaussian smoothing filter is fixed to 3×3 pixels and value of σ to 1.5. The average cputime time required for computing the feature vector (elements comprising of the fuzzy compactness value at three different thresholds) is 95.60 s. The experiment is performed in (SUN microsystems Ultra 60) system using MATLAB package.

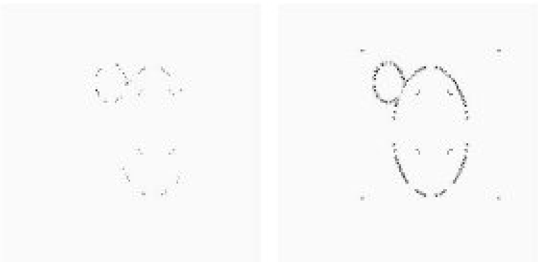

(a) (b)

Fig. 6. Edge candidates with $\mu_m(P) \geqslant 0.7$ connected to stronger pixels in 3×3 window with (a) $k_m = 1.18$ and k_d evaluated over 3×3 window. (b) $k_m = 1.18$ and k_d evaluated over 3×3 window. (Candidates with $\mu_m(P) \geqslant 0.7$ and $\mu_d(P) \geqslant 0.98$ for case (a) and $\mu_d(P) \geqslant 0.94$ in case (b) are plotted as crisp edge points.)

The experimental results are shown from Figs. 3–17. Fig. 3(a) is a synthetically generated image and its corresponding multilevel gradient map as obtained from Eq. (9) is shown in Fig. 4(a). The noisy version of the image is shown in Fig. 3(b). The corresponding gradient map is shown in Fig. 4(b). Figs. 5(a)–(c) shows the refined edge map of Fig. 3(a) at different threshold with ($\mu_m(P) \geqslant 0.6, 0.7, 0.8$). Fig. 5(d) is the refined edge map for the noisy image of Fig. 3(b). Considering Figs. 4(b) and 5(d) it is seen that the proposed technique has a good noise tolerance. Our aim is to select significant candidates from the multilevel edge map image containing meaningful shape and gray level information. From our proposed algorithm, it is observed from Fig. 4(a) that points of the curved regions are of lower membership value compared to the pixels belonging to the straight line. This property is used to extract points from curved regions of the edge map. In order to incorporate some less strong but significant edge points as candidates, we select those pixels which are having stronger pixels i.e. pixels of higher gradient membership $\mu_m(P)$ value over 3×3 window and $\mu_d(P)$ value of the concerned pixel $\simeq 1.0$. Such pixels of Fig. 3(a) are shown in Figs. 6(a) and (b). In case of Fig. 6(a) some pixels of sharp curvature are lost. However pushing down the threshold $\mu_d(P)$ it is possible to select some more pixels (pixels of sharp regions) as shown in Fig. 6(b). Such significant points of the bird and elephant image are also shown in Fig. 10 and corresponding original images are shown in Fig. 7. The refined edge map of the bird, deer image at $\mu_m(P) \geqslant 0.6$ is shown in Fig. 8. Fig. 8(a) shows that beside the edge points of the object, lot of edge points are generated from the background, which may result in a misleading characterization of the object by edge map. To reduce the effect of the background to some extent, a non-linear thresholding scheme is being used with

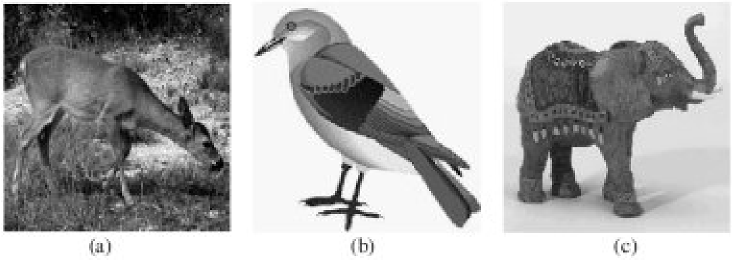

(a) (b) (c)

Fig. 7. Original images (a) deer image in textured background, (b) bird image and (c) elephant image.

varying the value of k_m of Eq. (9). which makes non-linear intensification of the edge membership value depending upon the value of k_m. We have performed two set of experiments to calculate feature values (feature sets (A) and (B)) described in Section 3, with varying the value of k_m and with different size of support window. Fig. 9(a) is obtained at $\mu_m(P) \geqslant 0.8$ using Eq. (9) and k_d evaluated from Eq. (12) with feature set (A). Fig. 9(a1) is obtained by thresholding at $\mu_m(P) \geqslant 0.8$ by choosing $k_m \simeq 1.18$ and k_d is evaluated from Eq. (12). Fig. 9(a2) is obtained by thresholding at $\mu_m(P) \geqslant 0.8$ by choosing $k_m \simeq 1.18$ and k_d is evaluated from Eq. (12) over 5×5 window size with feature set (B). It is evident from Fig. 9(a) that at higher threshold much of the significant edge points are lost. Better result is obtained from Fig. 9(a1) which can be explained from the following considerations. By non-linear intensification the pixels with higher membership values are more separated resulting enhancement. Such image can be thresholded at higher membership values preserving important edge information while rejecting some weaker edge pixels resulted from weak textured background. The result is further improved when larger size of the support window is used as shown in Fig. 9(a2). Fig. 11(a)–(c) shows the original image (bull image from trade mark database), it's edge map, and the edge map of the rotated image using feature set (B).

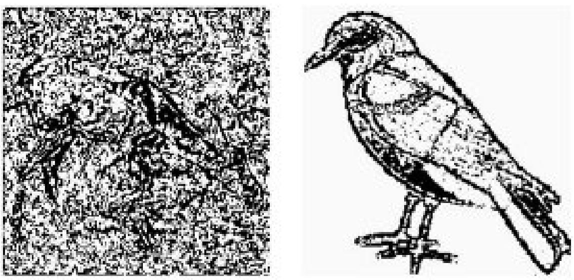

(a) (b)

Fig. 8. Edge map for candidates with $\mu_m(P) \geqslant 0.6$ and $\mu_d(P) \simeq 1.0$ plotted as crisp edge points. Value of k_d estimated over 3×3 window.

Feature values: The feature values (fuzzy compactness) of Fig. 12 are computed at different thresholds to study the invariance property of the feature which is used for indexing the images in our proposed method. The values are shown in Table 1. It is observed that the compactness value obtained for the translated and rotated version $(90°, 180°, 270°)$ gives satisfactory value. However the value differs by some amount for angle rotated at 30°. This can be explained from the fact that the popular image rotation algorithms suffers from digitization error due to interpolation, thereby influencing the feature values as seen from Fig. 12(c). The feature value of scaled version is changed by some amount due the reason mentioned above.

The image retrieval experiment is performed by computing features separately using feature sets (A) and (B). We select a particular image as query and based on the Euclidean distance computed using Eq. (13) the images are ranked according to the increasing order of distance. Top twenty images are selected. These results are shown in Figs. 13–17. Here the images are rankled left to right and top to bottom in increasing distance.

Retrieval of assorted gray level images (*database 1*): The experimental results are shown in Figs. 13, 14 and 15. The usefulness of the algorithm is represented here, to find images as a whole that appear visually similar, particularly for finding similar scenes, similar faces or objects from the data base.

Fig. 13(a) shows the results of the first twenty retrieved images with the query image on the top left corner. It is seen from Fig. 13(a) that the rotated and scaled version of the image, the noisy version of the image are the candidates retrieved at a higher rank.

Fig. 13(b) shows the result when queried with a tiger in a textured background. The global similarity measure (fuzzy compactness) works well here. The object(tiger) in this case constitutes a significant portion of the image. By non-linear intensification of the candidate pixels the effect of weak textured background is minimized to some extent. A good precision is obtained in this case.

Figs. 14(a) and (b) shows the experimental results when queried with the girl image. It should be noted that the

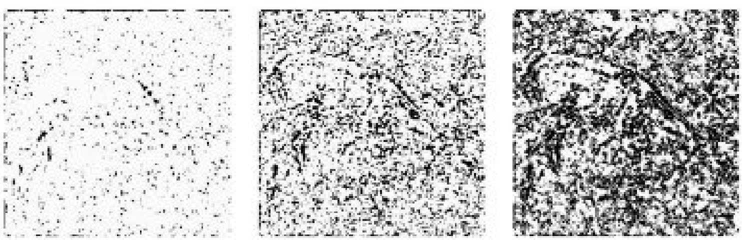

(a) (a1) (a2)

Fig. 9. (a) Edge map with value of k_d estimated over 3×3 window (feature set A). Enhanced edge map with $k_m = 1.18$. (a1). Value of k_d estimated over 3×3 window. (a2) k_d estimated over 5×5 window (feature set B). (Candidates with $\mu_m(P) \geqslant 0.8$ and $\mu_d(P) \simeq 1$ plotted as crisp edge points.)

system presented here works well for faces using the same representation parameters which has been used for other cases. Better precision is obtained with feature set (B) in which the strong edge pixels are more separated than the weak pixels by non-linear intensification of the pixels.

Figs. 15(a) and (b) shows the experimental results when queried with the bird image. The rotated, the noisy images, are retrieved at a higher rank. Also some background variation is tolerated. Better precision is obtained with feature set (B) in this case.

(a) (b)

Fig. 10. Edge candidates with $\mu_m(P) \geqslant 0.7$ connected to stronger pixels in 3×3 window with $k_m = 1.18$ and k_d evaluated over 3×3 window. (Candidates with $\mu_m(P) \geqslant 0.7$ and $\mu_d(P) \simeq 1$ plotted as crisp edge points.)

It is seen from Figs. 13–15 that there are few other dissimilar images retrieved at an higher rank. Such results can be explained considering the fact we have used a global measure (fuzzy compactness) for computing similarity. As the fuzzy compactness is computed from the edge map irrespective whether the pixel belongs to the object or background, the resultant compactness value can have contribution both from the object and background. In case when the background is textured the contribution from the background is more in comparison to the case where the background is uniform. This results in a higher degree of error in computing the compactness of the object of interest.

Retrieval of trademark images (*database 2*): Figs. 16 and 17 shows the performance of our algorithm on the trade mark images. It is difficult to judge the relevance in case of trade mark images because it is difficult to judge visually similar trade marks. In case of trade mark images, color or gray level contrast information doesnot play a useful role in distinguishing between various marks. The searching of the trade mark image is based mostly on the decision of the shape information present in the binary images. Therefore the recall and precision can be subjected to some error.

Fig. 16(a) shows the retrieval performance when queried with the image on the top left corner. Most of the retrieved images have almost the same structure. The first five successive images depicts the rotated version of the query

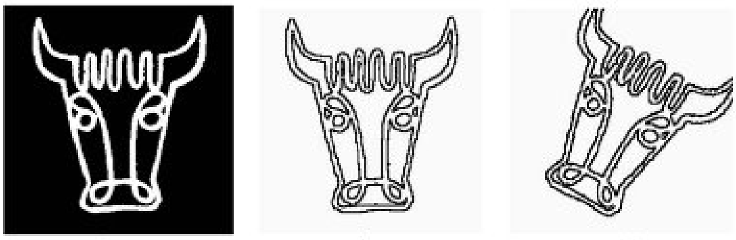

(a) (b) (c)

Fig. 11. (a) Original image, (b) edge map and (c) edge map of rotated image. Edge candidates with $\mu_m(P) \geqslant 0.7$ with $k_m = 1.18$ and k_d evaluated over 3×3 window. (Candidates with $\mu_m(P) \geqslant 0.7$ and $\mu_d(P) \simeq 1$ plotted as crisp edge points.)

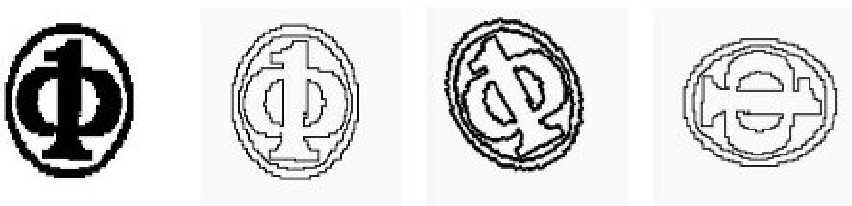

(a) (b) (c) (d)

Fig. 12. (a) Original image, (b) Edge map, (c) Rotated edge map (30°), (d) Rotated edge map (90°). Edge candidates with $\mu_m(P) \geqslant 0.7$ with $k_m = 1.18$ and k_d evaluated over 3×3 window. (Candidates with $\mu_m(P) \geqslant 0.7$ and $\mu_d(P) \simeq 1$ plotted as crisp edge points.)

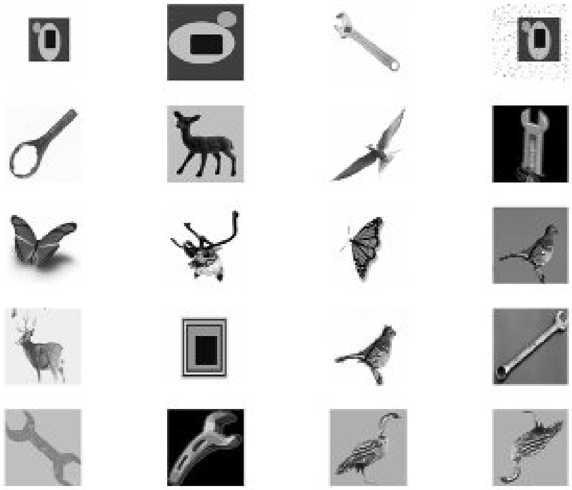

(a)

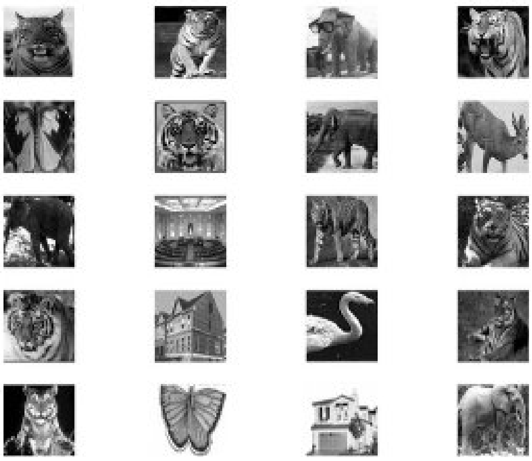

(b)

Fig. 13. Retrieved result, with top left image as the query image. (a) using feature set (A) and (b) using feature set (B).

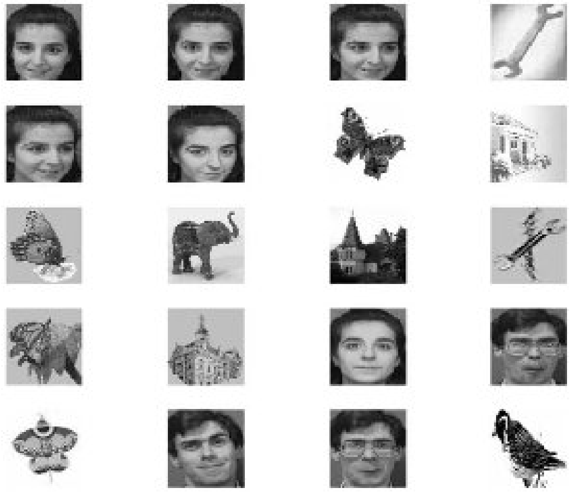

(a)

(b)

Fig. 14. Retrieved result, with top left image as the query image. (a) using feature set (A) and (b) using feature set (B).

image. It is seen that the shape characteristics of the image is adequately captured by our approach in this case.

Fig. 16(b) shows the performance with the query image on the top left corner. The translated and the rotated versions of the image are retrieved at a rank within the first twenty retrieved images.

Fig. 16(c) shows the performance with the query image of a bull's head. The images rotated at different angles are retrieved within the first twenty ranked images. However there are few other images retrieved at an higher rank.

Fig. 17 shows the performance with the query image on the top left corner. The image rotated at different angles are retrieved at a rank within the first forty retrieved images. However certain images differing in shape with the query image but having approximately close feature value are also retrieved at a higher rank.

It is observed from our experimental result of Figs. 16 and 17 that some dissimilar images attains higher rank and comes between similar images. This can be explained from the fact that the refined edge map which is obtained by taking the degree of linking is based on the turning edge angles of the object boundary. Such shape features give accurate results with objects having one closed boundary. Practical images have many fine details and turning angle features. This may reduce the precision to some extent.

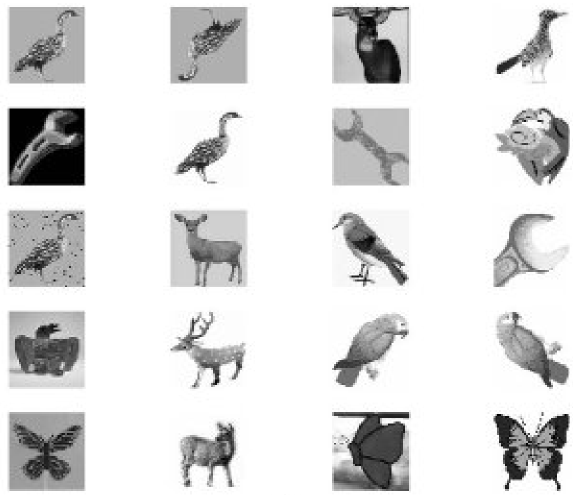

(a)

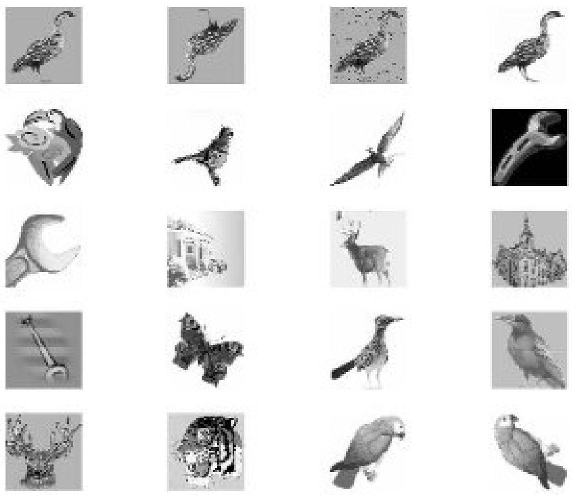

(b)

Fig. 15. Retrieved result, with top left image as the query image. (a) using feature set (A) and (b) using feature set (B).

4.1. Performance measure

In our experiment the relevant images are decided in advance. The performance measure is judged from the recall rate and precision rate obtained from the first twenty successively retrieved images. Values are shown in Table 2. Either value alone contains insufficient information. Precision can be made high by retrieving only few images and recall can be made equal to 1 simply by retrieving all images [19].

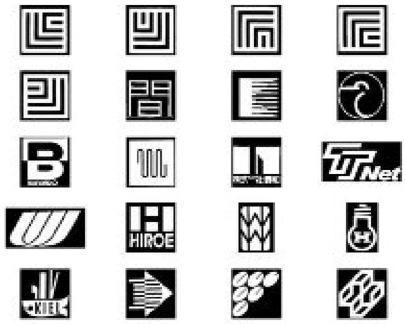

(a)

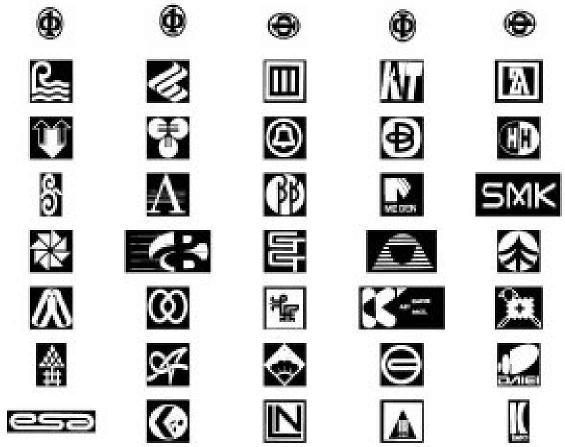

(b)

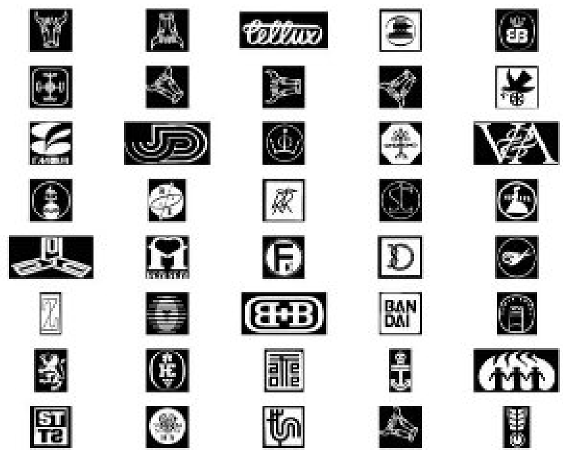

(c)

Fig. 16. Retrieved result, using feature set (B) with top left image as the query image (USPTO) database.

5. Conclusion

As is evident from the experimental results fuzzy compactness provides an fairly good tool for indexing and can be able to retrieve similar images from a heterogeneous database whose classes are not known apriori. Fuzzy compactness feature is computed from the edge map containing edge points only. Number of edge points are a small fraction of the total number of pixels in an image. It is an inexact method and its performance is best achieved when queried with single objects and having non textured background. The method could be further improved if we use some other features like moment in association with the present work. This work is being tried in our laboratory to improve the search accuracy.

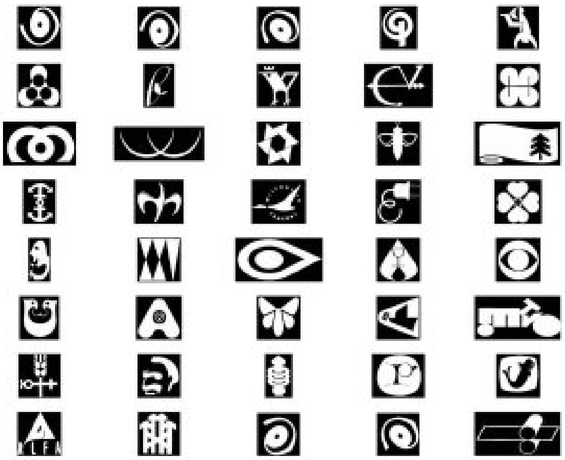

Fig. 17. Retrieved result, using feature set (B) with top left image as the query image (USPTO) database.

Table 1
Feature values

Image	$comp(\mu_1)$	$comp(\mu_2)$	$comp(\mu_3)$
Fig. 12 (0°)	0.000184	0.000184	0.000129
Fig. 12 (translated)	0.000184	0.000184	0.000129
Fig. 12 (scaled)	0.000140	0.000140	0.000078
Fig. 12 (90°)	0.000184	0.000184	0.000131
Fig. 12 (180°)	0.000184	0.000184	0.000131
Fig. 12 (30°)	0.000150	0.000134	0.000134

6. Summary

This paper presents a robust technique for extracting edge map of an image which is followed by computation of global feature (like fuzzy compactness) using gray level as well as shape information of the edge map. Unlike other existing techniques it does not require pre segmentation for the computation of features. This algorithm is also computationally attractive as it computes different features with limited number of selected pixels. The common problem in Content Based Image Retrieval (CBIR) is selection of features. Image characterization with lesser number of features involving lower computational cost is always desirable. Edge is a strong feature for characterizing an image. Although minimum number of features are always desirable property for characterizing images but single features may not be sufficient for achieving desired accuracy. Color and texture based similarity measures without shape information failed to produce desired results. It is also desirable that, the selected features should not be computationally expensive, should be noise tolerent and invariant to rotation, translation and scaling. We have used the blurred image as input and used the concept of Top and Bottom of the intensity surface to extract possible candidates for the edge map. By gaussian filtering, part of the intensity is distributed to the neighbours while preserving the edge information. The border region which characterizes the transition between two uniform Plateaus could be determined from the blurred image. We are interested in finding the transition between the Plateau regions consisting of the possible edge candidates which acts as an input for finding the fuzzy gradient map. The fuzzy gradient map is obtained by measuring the relative intensity difference over small neighbourhood. The pixels are categorized as Weak, Medium, Strong based on their contrast membership value. Multilevel thresholding above certain membership value is performed to find multilevel fuzzy edge map, from which (fuzzy compactness vector) is computed. The feature vector elements include fuzzy compactness value of the edge map obtained at different level which is used to compute the degree of similarity measure of an image with the query image for image retrieval. This geometrical

Table 2
Performance evaluation %

Image	$n_1(A)$	$n_1(B)$	n_2	Rec.rate(A)	Pr.rate(A)	Rec.rate(B)	Pr.rate(B)
Fig. 14 (girl)	6	9	10	60	30	90	45
Fig. 15 (bird)	8	11	11	72	40	100	55
Fig. 13(b) (tiger)		9	12			75	45
Fig. 13(a) (square)	4		4	100	20		
Fig. 16(a) (logo)		9	12			73	45
Fig. 16(b) (logo)		8	10			80	40
Fig. 16(c) (logo)		7	10			70	35
Fig. 17 (logo)		8	13			56	40

feature is invariant to Rotation Translation and Scaling by definition and physically means the maximum area that can be encircled by the perimeter. The similarity between the feature vectors of two images are computed by the widely used standard Euclidean distance metric.

References

[1] A.W.M. Smeulders, M. Worring, S. Santini, A. Gupta, R. Jain, Content-based image retrieval at the end of the early years, IEEE Trans. Pattern Anal. Mach. Intelligence 22 (12) (2000) 1349–1380.

[2] V.N. Gudivada, V.V. Raghavan, Content based image retrieval systems, IEEE. Comput. 28 (9) (1995) 18–22.

[3] A.K. Jain, Vailaya, Image retrieval using color and shape, Pattern Recognition 29 (1996) 1233–1244.

[4] X.S. Zhou, T.S. Huang, Edge-based structural features for content-based image retrieval, Pattern Recognition Lett. 22 (2001) 457–468.

[5] J. Wang, R. Gray, G. Wiederhold, System for screening objectionable images, Comput. Commun. J. 21 (15) (1998) 1355–1360.

[6] S. Ravela, R. Manmatha, W. Croft, Retrieval of trademark and gray-scale images using global similarity (1998). URL citeseer.nj.nec.com/ravela98retrieval.html

[7] L. da Fontoura costa, R. Marcondes, Shape analysis and classification, CRC Press, USA, 2001.

[8] O. Bruno, R. Cesar, L.A. Consularo, Automatic feature selection for biological shape classification in synergos, SIBGRAPI-98, IEEE. Comput. Society Press, 1998, pp. 363–370.

[9] T. Gevers, A.W.M. Smeulders, Combining color and shape invariant features for image retrieval, Image Vision Comput. 17 (7) (1999) 475–488.

[10] C. Achard, J. Devars, L. Lacassagne, Object image retrieval with image compactness vectors, 15th International Conference on Pattern Recognition, Bercelona, Spain, 2000, pp. 271–274.

[11] J.K. Udupa, G.J. Grevera, Go digital, go fuzzy, Pattern Recognition Lett. 23 (2002) 743–754.

[12] L.A. Zadeh, Fuzzy sets, Inform. Control 8 (1965) 338–353.

[13] S.K. Pal, D.D. Majumder, Fuzzy Mathematical Approach to Pattern Recognition, Wiley Eastern Limited, New York, 1985.

[14] A. Rosenfeld, Fuzzy digital topology, in: J.C. Bezdek, S.K. Pal (Eds.), Fuzzy Models for Pattern Recognition, IEEE Press, New York, 1991, pp. 331–339.

[15] S.K. Pal, A. Rosenfeld, Image enhancement and thresholding by optimization of fuzzy compactness, in: J.C. Bezdek, S.K. Pal (Eds.), Fuzzy Models for Pattern Recognition, IEEE Press, New York, 1991, pp. 369–379.

[16] B.B. Chaudhury, B.U. Shankar, An efficient algorithm for extrema detection in digital images, Pattern Recognition Lett. 10 (1989) 81–85.

[17] R.C. Gonzalez, R.E. Woods, Digital Image Processing, Wiley, New York, 1985.

[18] A.D. Bimbo, Visual Information Retrieval, Morgan Kaufmann Publishers, Inc., San Francisco, USA, 2001.

[19] H. Muller, W. Muller, D. Squire, S.M. Maillet, T. Pun, Performance evaluation in content-based image retrieval: overview and proposals, Pattern Recognition Lett. 22 (2001) 593–601.

About the Author—MINAKSHI BANERJEE received her B. Tech., M. Tech. in Radio Physics and Electronics in 1990 from the University of Calcutta. In 1992, she joined as a Technical Officer in Government of India and worked upto 1993. She had been working as a System specialist in a software company (India Infopower International Pvt. Ltd.) and worked in different projects. Presently she is a Senior Research fellow of Council of Scientific and Industrial Research and doing doctoral degree at the Machine Intelligence Unit of the Indian Statistical Institute.

About the Author—MALAY K. KUNDU received his B. Tech., M. Tech. and Ph.D. (Tech.) degrees all in Radio Physics and Electronics from the University of Calcutta. In 1982, he joined the Indian Statistical Institute, Calcutta, as a faculty member. He had been the Head of the Machine Intelligence Unit of the Institute during September 1993 to November 1995 and currently he is a full professor of the same unit. During 1988–1989, he was at the A.I. Laboratory of the Massachusetts Institute of Technology, Cambridge, U.S.A., as a visiting scientist under U.N. Fellowship program. His current research interest includes image processing & analysis, image compression, machine vision, genetic algorithms, fractals, wavelets, VLSI design for digital imaging. and soft computing. He received the prestigious VASVIK award for industrial research (Indian equivalent of the Mullard award of U.K.) in Electronic Sciences & Technology for the year 1999. He also received the Sir J. C. Bose memorial award from Institute of Electronics and Telecommunication Engineers (IETE), India in the year 1986. He has contributed about 70 research papers in well known & prestigious archival journals, international refereed conferences and as chapters in monographs & edited volumes. He is co author of the book titled *Soft Computing for Image Processing* published from Physica-Verlag, Heidelberg.

He is a senior member of the IEEE, USA, a *fellow of the National Academy of Sciences, India* and a *fellow of the Institute of Electronics and Telecommunication Engineers, India.*